Environmental Science
Processes & Impacts

Accepted Manuscript

ROYAL SOCIETY OF CHEMISTRY

rsc.li/process-impacts

Effects of pH and dissolved oxygen on the photodegradation of 17α-ethynylestradiol in dissolved humic acid solution

Dong Ren, Bin Huang, Tingting Bi, Dan Xiong, Xuejun Pan*

Faculty of Environmental Science and Engineering, Kunming University of Science and Technology, Kunming, Yunnan 650500, China

Abstract: To probe the mechanisms responsible for pH and dissolved oxygen (DO) affecting the photodegradation of EE2 in dissolved humic acid (HA) solution, EE2 aqueous solutions with pH ranging from 3.0 to 11.0 and different DO conditions were irradiated by a 300 W mercury lamp equipped with 290 nm light cutoff filters. In 5.0 mg L^{-1} HA solutions (pH 8.0), EE2 was degraded at a rate of 0.0739 h^{-1} which was about 4-fold faster than that in Milli-Q water. The degradation of EE2 was mainly caused by the oxidation of photogenerated reactive species (RS), and the contribution of direct photodegradation to EE2 degradation was always lower than 27%. Both the direct and indirect photodegradation of EE2 were closely dependent on the EE2 initial concentration, pH value and DO concentration. The photodegradation rate of EE2 decreased with increased initial concentration of EE2 due to the limitation of photon flux. With pH and DO increasing, the degradation rate of EE2 increased significantly due to the increase in the yields of excited EE2 and RS. Among the photogenerated RS, HO· and ^{3}HA* were determined to be the key contributors, and their global contribution to EE2 photodegradation was about 50%. Although HA could generate more $^1O_2$ than

* Corresponding author

E-mail address: xjpan@kmust.edu.cn

HO·, the contribution of $^1O_2$ to EE2 degradation was lower than 13% due to its low reactivity towards EE2. This study could enlarge our knowledge on the photochemical behaviors of steroid estrogens in natural sunlit waters.

Keywords: sensitized degradation; photodegradation; humic acid; environmental factor; 17α-ethynylestradiol

1. Introduction

17α-ethynylestradiol (EE2) has been widely used as an active component in oral contraceptive pills and discharged into aquatic systems by the effluent of wastewater treatment plants.[1,2] EE2 accumulated in waters may lead to some serious hazards to ecosystem and human endocrine system due to its strongest estrogenic potency among the steroid estrogens.[3-6] Thus, the fate and behaviors of EE2 in the natural aquatic systems has been attracted a global concern.[7,8] Among the various fates of environmental estrogens, the photodegradation was identified as one of the predominant removal approaches from natural waters.[9] The photodegradation half-life of EE2 was documented less than 2 days in lake water,[10,11] whereas EE2 was reported to be resistant to biodegradation with a half-life of 108 days under aerobic conditions,[9,12] and a longer lag stage could be expected under anaerobic conditions.[13,14]

The rapid photodegradation of EE2 in natural waters was always attributed to the acceleration effects of a number of organic and inorganic chromophores, such as the colored dissolved organic matter (CDOM), Fe(III)-organic complexes, nitrate and nitrite ions.[9] The ubiquitous of CDOM in aquatic systems is a heterogeneous mixture of aromatic and aliphatic organic compounds, mainly humic substances. Humic acid (HA), a main ingredient of humic substances, has been found to be of

distinctive potential in accelerating the photodegradation of pollutants,[15] and the acceleration function of HA has been attributed to the photogenerated reactive species (RS).[16,17] HA can typically absorb the photons in the range of 300-500 nm solar spectrum forming short-lived RS (^{1}HA*) by the unsaturated conjugated structures and free electron pairs on heteroatoms.[18] The ^{1}HA* may fragment into smaller molecular, go back to the ground state by losing energy or interacting with quenching reagents, and undergo an inter-system crossing process forming triplet-excited photosensitizer (^{3}HA*).[19] Furthermore, the formed ^{3}HA* can react with molecular oxygen and other chemicals to generate the secondary reactive oxygen species (ROS), including hydroxyl radical (HO·), singlet oxygen ($^1O_2$), hydrogen peroxide (H_2O_2) and superoxide anion ($O_2^{\cdot-}$).[16,20,21]

Previous studies reported that the photodegradation of steroid estrogens was significantly enhanced by HA acting as a photosensitizer,[9-11,22] and this role always varied across waters due to the special components and aquatic characteristics. Among the extensive aquatic characteristics, dissolved oxygen (DO) and pH were two important parameters since they could participate the process of ROS formation[9] and change the speciation of EE2 and HA.[10,18] It was also documented that photooxidation rate of DOM would be increased in acidified streams relative to that in neutral pH.[23] However, the pathways and mechanisms responsible for DO and pH affecting the direct photodegrdation of EE2 and the photodegadation of EE2 mediated by HA remain unclear. Furthermore, to the best of our knowledge, the information on the photogenerated RS affecting EE2 degradation is still very limited, including the formation pathways of RS, individual contribution of RS to EE2 degradation and the reaction potency of the main RS towards EE2.

This study is devoted to quantify the contribution of direct photodegradation and RS produced by a

local HA to the degradation of EE2, and to explore the mechanisms responsible for water characteristics, DO and pH, affecting the photogeneration of RS and the photodegradation of EE2 in Milli-Q water and HA aqueous solutions. This study can further our knowledge on the photochemical behaviors of steroid estrogens in natural waters and provide information on the feasibility of incorporating the photodegradation technology into wastewater treatment plants in the near future.

2. Materials and methods

2.1. Chemicals

EE2, i-PrOH (IPA), furfuryl alcohol (FFA), terephthalic acid (TPA), 2-hydroxyl terephthalic acid (2-hTPA), catalase (CAT), sorbic acid (SA), rose bengal (RB) and benzoic acid (BZA) were purchased from Sigma Aldrich (USA). Selected physicochemical properties of EE2 are shown in Table 1. H_2O_2, $FeSO_4 \cdot 7H_2O$ and H_2SO_4 were purchased in analytical grade from Sinopharm Chemical Reagent Co., Ltd., China. Milli-Q water (electric resistivity > 18 MΩ cm) was used throughout this study. The used HA was extracted from the sediment collected from Dianchi Lake (centered around 24°48′2″ N, 102°40′17″ E) by a previously reported method[16] with some modifications. The sediment collection information and HA extraction procedures were shown in Text S1 of electronic supplementary material.

<Table 1>

2.2 Solution preparation

EE2 working solution was prepared freshly every week. 5.00 mg EE2 was added into 1 L Milli-Q water followed by continuously stirred for 24 h at room temperature to ensure a maximum dissolution, and then the supernatant was collected by passing through 0.45 μm glass fiber filters (GF/F, Millipore

Corp., USA) which were prebaked for 4 h at 450 °C. Prepared working solutions were stored at 4 °C in brown glass bottles wrapped with aluminum foil to avoid photodegradation.

HA stock solution was obtained by dissolving 500 mg HA powder in about 500 mL NaOH solution (0.05 M). After being stirred for 24 h at room temperature, the solution was centrifuged at 2327 *g* for 15 min and filtered by prebaked GF/F to remove insoluble particles. The prepared HA stock solution was stored in a polyethylene container and kept at 4 °C in dark conditions for using within 3 weeks.

2.3. Photodegradation experiments

Batch photochemical experiments were performed on an XPA-7 merry-go round photochemical reaction apparatus shown in Figure S1a. All cylindrical quartz reactors (with a volume of 50 mL and a diameter of 15 mm) were stirred by a magnetic stirrer and illuminated by a 300 W medium pressure mercury lamp equipped with 290 nm light cutoff filters. The emission spectrum of the light source was displayed in Figure S1b and the light intensity was determined to be 3.71 mW m^{-2} at 365 nm and 21.6 mW m^{-2} for $\lambda > 420$ nm, respectively. These light intensities were measured by an ultraviolet and a visible light irradiation detector (Photoelectric Instrument Factory of Beijing Normal University, China) at the surface of the reactors away from the light source 5.5 cm.

EE2 degradations (40 mL, 1.24 mg L^{-1}) were performed at 23 ± 0.5 °C which was controlled by a recirculating cooling water bath. Before being irradiated, all the solutions were adjusted pH to the desired values by adding 1.0 M NaOH and 1.0 M H_2SO_4, and then equilibrated in dark for 1 h. Change in pH value for all degradations was measured by a UB-7 pH meter at the end of each irradiation period, which indicated that the extent of the changes was always lower than 0.1. In order to explore the roles of pH and DO acted in EE2 photodegradation, batch experiments were performed

as follows: (1) Stability of EE2 was tested in Milli-Q water, 0.05 M $NaHCO_3$ and HA aqueous solutions under dark and irradiation conditions, respectively; (2) HA-dependent photodegradation of EE2 was tested in a HA concentration range of 0 - 20 mg L^{-1}, and pH-dependent photodegradation of EE2 were performed within a pH range of 3.0 - 11.0; (3) DO-dependent photodegradation of EE2 was performed in N_2 or O_2 purging systems, and the photodegradation of EE2 in the systems exposed to air was taken as reference; (4) RS scavenging experiments were performed by adjusting the solutions containing 2% (v/v) IPA, 0.2 mM FFA, 0.5 mM SA and 0.015 mg mL^{-1} CAT to trap HO·, $^1O_2$, ^{3}HA* and H_2O_2, respectively;[26-29] (5) Steady-state concentration of HO· and $^1O_2$ was measured by TPA and FFA (Text S2, Figure S2 and Figure S3), respectively; (6) Reaction rate constant between HO· and EE2, and that between $^1O_2$ and EE2 was detected by competition kinetics method,[30] by taking H_2O_2/Fe^{2+} and rose bengal as the source of HO· and $^1O_2$, respectively (Text S3, Table S1, Table S2, Figure S4 and Figure S5). All photochemical experiments were conducted in duplicate.

2.4. Sample Analysis

Aliquots of 500 μL samples were withdrawn from irradiated solutions at different time intervals and quantified EE2 residual on a high performance liquid chromatography (HPLC, Agilent Technologies 1260) by the method shown in Table S3. The detection limit of EE2 was determined to be 0.02 mg/L, and the relative standard deviation for all samples was within 5%. Quantifications for BZA, FFA, and 2-hTPA were also performed on the HPLC which was equipped with a CORTECS™ C18 column (2.7 μm, 4.6 mm × 100 mm) and a UV-fluorescence dual detector. Detail information on the detection methods was also depicted in Table S3.

HA was characterized for fluorescent, elemental, and light absorption properties by a fluorescence

spectrophotometer (Perkin Elmer, LS55), an elemental analyzer (Elementar, MicroCube), and a UV-vis spectrometer (SHIMADZU, 2600), respectively. The detected results and calculated indices of HA were shown in Figure S1c, Figure S1d and Table S4. Concentration of HA in all aqueous solutions was quantified by a TOC analyzer (Elementar, Vario TOC APSA-370).

3. Results and discussion

3.1. Direct photodegradation of EE2

3.1.1 Stability of EE2 in solution

Dark controls in Milli-Q water and 0.05 M $NaHCO_3$ were performed to identify the stability of EE2. As shown in Fig. 1, EE2 was quantitatively recovered (> 95%) in dark controls, which indicated that hydrolysis, volatilization, and sorption onto the walls of quartz tubes were not the significant contributors to EE2 loss when it was photodegraded.

EE2 can be degraded slowly in Milli-Q water at pH 8.0 ± 0.1 under the irradiation of the simulated sunlight source (Fig. 1), which is due to its weak light absorption in the wavelength of 290-320 nm. Plot of $\ln(C/C_0)$ versus irradiation time t displays a linear relationship with an adjusted correlation coefficient (r_{adj}^2) of 0.9929 calculated by Eqs. (1) and (2), which indicates that the direct photodegradation of EE2 follows pseudo-first-order kinetics.

$$\ln(C / C_0) = k_{obs} t \qquad (1)$$

$$r_{adj}^2 = 1 - [(1 - r^2)(\mathrm{m} - 1) / (\mathrm{m} - \mathrm{b} - 1)] \qquad (2)$$

where C and C_0 are the concentration of EE2 at photoreaction time t and time zero in h, respectively; k_{obs} is the observed pseudo-first-order rate constant in h^{-1}; r^2 is the regression coefficient of the linear fitting; m and b in Eq. (2) are the number of experimental data points and parameters, respectively.

<Fig. 1>

To assess the direct photodegradation efficiency of EE2 in the wavelength range of 290 - 320 nm, phenol was selected as a chemical actinometer because it shares a similar light absorption characteristics with EE2 (Figure S1d). The quantum yield of EE2 ($\phi^{EE2}_{290\text{-}320}$) was calculated by the reported methods[31,32] and Eq. (3) with a step of 0.5 nm which was built on the observed pseudo-first order rate constant of EE2 and phenol as Eq. (4) and (5). According to the observed photodegradation rate of EE2 0.0193 ± 0.0003 h^{-1}, the quantum yield was calculated as 0.0102 ± 0.0002 mol $einstein^{-1}$. Compared to the photodegradation of most fluoroquinolone antibiotics (varied from 0.0047 mol $einstein^{-1}$ for enrofloxacin to 0.0697 mol $einstein^{-1}$ for gatifloxacin),[17] estrone (0.0246 mol $einstein^{-1}$)[34] and 17β-estradiol (0.07 mol $einstein^{-1}$)[32] in pure water, EE2 is a relative photo recalcitrant chemical. Therefore, EE2 may accumulate in aquatic systems and exhibit hazardous to human and wildlife due to its longer half-life (about 36 h, calculated by dividing ln2 by the rate constant) and higher estrogenic potency than other pharmaceuticals, estrogens and personal care products[3,6].

$$\phi^{EE2}_{290\text{-}320} = \phi^{phenol}_{290\text{-}320} \times \frac{k^{EE2}_{obs}}{k^{phenol}_{obs}} \times \frac{\sum_{290}^{320} I_\lambda \varepsilon^{phenol}_\lambda}{\sum_{290}^{320} I_\lambda \varepsilon^{EE2}_\lambda} \qquad (3)$$

$$k^{EE2}_{obs} = 2.303 l \phi^{EE2}_{290\text{-}320} \sum_{290}^{320} I_\lambda \varepsilon^{EE2}_\lambda \qquad (4)$$

$$k^{phenol}_{obs} = 2.303 l \phi^{phenol}_{290\text{-}320} \sum_{290}^{320} I_\lambda \varepsilon^{phenol}_\lambda \qquad (5)$$

where $\phi^{EE2}_{290\text{-}320}$ (mol $einstein^{-1}$) is the quantum yield of EE2 in the wavelength range of 290 - 320 nm; $\phi^{phenol}_{290\text{-}320}$ is the quantum yield of phenol, which was reported to be 0.03 mol $einstein^{-1}$ with λ > 290 nm;[33] k^{EE2}_{obs} and k^{phenol}_{obs} are the observed photodegradation rate constant of EE2 and phenol in h^{-1}, respectively; I_λ (einstein L^{-1} s^{-1}) is the photon flux rate at the wavelength λ; ε_λ (M^{-1} cm^{-1}) is the molar

absorption coefficient of EE2 or phenol.

3.1.2 Effects of EE2 initial concentration

The effect of EE2 initial concentration on the direct photodegradation was tested at pH 8.0 ± 0.1 with a concentration range of 0.1 - 3.0 mg L^{-1}. As shown in Fig. 2, all the photodegradations followed pseudo-first-order kinetics, and r_{adj}^2 for all linear regressions was higher than 0.95. The direct photodegradation of EE2 was significantly inhibited by the increased initial concentration (about a 51% reduction in rate constant for a 8-fold increase in initial concentration), and the half-life of EE2 ranged from 18.5 to 37.6 h within the concentration range of 0.1 - 0.8 mg L^{-1}. EE2 in natural waters was usually detected at nM or pM level,[2] which indicated that EE2 would have a far shorter half-life in natural waters than that discussed here. The photodegradation of EE2 in Milli-Q water tended to be stable when its concentration higher than 0.8 mg L^{-1}. Similar results were also reported in the photodegradation of estrone and estriol[34,35]. The decrease in the direct photodegradation rate of EE2 might be related to the limitation of incident photons and the light screening effect. To assess this, the measured rate constants of EE2 at higher concentrations were corrected by light screening effect according to the reported methods[21] and Eqs. (6) and (7). The corrected rate constant of EE2 (k_{cor}) ranged from 0.0374 to 0.0369 h^{-1}, which was compatible with that at 0.1 mg L^{-1} (0.0375 h^{-1}). Therefore, the decrease in the photodegradation rate of EE2 was indeed caused by the light screening effect.

$$k_{cor} = k_{EE2} \times \frac{(I_a/I_0)_{EE2/EE2'}}{(I_a/I_0)_{EE2}} \qquad (6)$$

$$(I_a/I_0)_{EE2/EE2'} = (I_a/I_0)_{EE2'} \times (A_{EE2}/A_{EE2'}) \qquad (7)$$

where, $(I_a/I_0)_{EE2/EE2'}$ is the fraction of light absorbed by EE2 at the concentration of 0.1 mg L^{-1} and

at 292 nm; $(I_a/I_0)_{EE2'}$ is the fraction of light absorbed by EE2 at the concentration higher than 0.1 mg L^{-1} and at 292 nm; A_{EE2} and $A_{EE2'}$ are the absorbance of 0.1 mg L^{-1} EE2 and higher at 292 nm, respectively; k_{EE2} is the photodegradation rate constant of EE2 at 0.1 mg L^{-1} in h^{-1}.

<Fig. 2>

3.1.3 Effects of pH on the direct photodegradation of EE2

Experiments were performed at different pH values of 3.0, 5.0, 7.0, 8.0, 9.0 and 11.0 to determine the influence of pH on the direct photodegradation of EE2. The photodegradation kinetics and quantum yield of EE2 were closely dependent on pH condition and reached the lowest value at pH 7.0 (Fig. 3). After 6 h irradiation, 25%, 10% and 90% of EE2 were degraded in the solution at pH 3, 7 and 11, respectively. Higher photodegradation rate of EE2 in strong alkaline solution could be explained by taking the dissociation of EE2 and the changes in UV-vis absorption characteristics of EE2 into consideration (Fig. 4). A significant fraction of EE2 was deprotonated at pH 11.0 due to the p*K*a value reported to be 10.5 for EE2.[24] Furthermore, the deprotonated organic chemicals were always reported to be more sensitive to light,[36] whereas the protonated chemicals were less.[37,38] Thus, the photodegradation rate at pH 11.0 was much higher than that at lower pH value. It is noteworthy that a higher degradation rate of EE2 in strong acidic aqueous solution could also be expected compared to that in the neutral, weak acidic, and weak basic solution. This result was in line with the influence of pH on direct photodegradation of 17β-estradiol and estrone aqueous solution irradiated by a UV-vis light source.[39]

<Fig. 3>

<Fig. 4>

3.2. Photodegradation of EE2 in the presence of HA

3.2.1 The photodegradation of EE2 induced by HA

HA is ubiquitous in natural waters, and it is a major RS source,[40] an incident light screen,[41] and a RS scavenger.[30] To investigate the effect of HA on EE2 photodegradation, EE2 degradations (1.24 mg L^{-1}) were performed in the solutions contained 5.0 mg L^{-1} HA. As shown in Fig. 1, HA could effectively induce EE2 photodegradation at a rate about 4-fold faster than that in Milli-Q water, which was in line with previous reported results[11,22]. HA could always act dual roles in the photodegradation of organic pollutant, i.e., promoter and inhibitor.[42] Thus, the influence of HA concentration on EE2 photodegradation was performed with HA ranging from 0 to 20 mg L^{-1} (table 2). The photodegradation rate of EE2 in HA containing solutions was dramatically enhanced compared to that in Milli-Q water. However, HA could inhibit the degradation of EE2 when it exceeded the critical concentration of 10 mg L^{-1}. Similar phenomenon was also found in the study of HA inducing 17β-estradiol photodegradation.[43] The inhibition effect of HA on the photodegradation of organic pollutants was always attributed to its competing incident light and scavenging RS functions.[17,26,30] To explore the mechanisms responsible for the inhibition effect of HA on the photodegradation of EE2, degradation rate constants were corrected by light screening effect of HA as Eq. (6) with minor modifications. As listed in table 2, the corrected rates were always lower than 0.0193 h^{-1} and decreased steadily with increased concentration of HA, which indicated that both light screening and RS scavenging mechanisms were involved in the photodegradation of EE2 in HA solutions.

<Table 2>

3.2.2 Influence of pH on the photodegradation of EE2 induced by HA

In order to explore the influence of pH on the photodegradation of EE2 induced by HA, EE2 was irradiated in the solutions containing 5.0 mg L^{-1} HA with pH ranging from 3.0 to 11.0. As shown in Fig.5, the pH-dependent photodegradation rate of EE2 decreased to the minimum value of 0.0587 h^{-1} at pH 5.0, while the lowest degradation rate of EE2 in Milli-Q water was found at pH 7.0. HA was reported to be a heterogeneous mixture and a weak acidic polyelectrolyte.[44] Therefore, HA might be in ionized state when pH exceeded 5.0, and the deprotonated HA could absorb more incident light (Figure S6) and produce more RS.[23] As a result, the photodegradation rate of EE2 increased with pH increased from 5.0 to 11.0. The degradation rate of EE2 at pH 3.0 was found to be higher than that at pH 5.0, which was also related to the influence of hydrogen ion on the RS formation.[23] In general, the effect of pH on the photodegradation of EE2 in HA solution was minor than that in Milli-Q water.

<Fig. 5>

3.3. Role of DO in EE2 photodegradation

In order to explore the influence of DO on the photodegradtion of EE2 in the presence and absence of HA, nitrogen and oxygen were bubbled into solutions for providing a DO condition of 0.4 mg L^{-1} and 7.1 mg L^{-1}, respectively. The concentration of DO in the solutions exposed to air was measured to be 3.8 mg L^{-1}, and the photodegradation of EE2 in those systems was taken as reference. A quantitative comparison of EE2 photodegradation kinetics in the presence and absence of DO was shown in Fig. 6. The photodegradation rate of EE2 was slightly inhibited in the Milli-Q/N_2 system (0.0178 h^{-1}) compared to that in the Milli-Q/Air system (0.0193 h^{-1}), whereas the degradation of EE2 in the HA/N_2 system (0.0539 h^{-1}) was inhibited by 27% compared to that in the HA/air system (0.0739 h^{-1}). The degradation of EE2 in oxygen enriched systems, however, could be dramatically enhanced, and

the rates increased to 0.0477 and 0.1674 h^{-1} for Milli-Q/O_2 and HA/O_2 system, respectively. The pathways of DO promoting the photodegradation of organic pollutant could be typically summarized as follows: (i) promoting the further oxidation of the photochemical intermediates and products,[36] (ii) reacting with photosensitizers producing $^1O_2$, HO· and H_2O_2,[16,20] and these ROS were identified as the key contributors to the degradation of organic pollutant.[45,46] Thus, the pathways for DO enhancing EE2 photodegradation could be proposed as Eqs. (8) - (14).

$$EE2 + h\nu \xrightarrow{O_2} \text{Products} \quad (8)$$

$$HA + h\nu \rightarrow {}^3HA^* \quad (9)$$

$${}^3HA^* + O_2 \rightarrow {}^1O_2 + HA \quad (10)$$

$${}^3HA^* + O_2 \rightarrow O_2^{\cdot-} + HA^+ \quad (11)$$

$$2O_2^{\cdot-} + 2H^+ \rightarrow H_2O_2 + O_2 \quad (12)$$

$$H_2O_2 + h\nu \rightarrow 2HO^{\cdot} \quad (13)$$

$${}^3HA^* / {}^1O_2 / HO^{\cdot} + EE2 \rightarrow \text{Products} \quad (14)$$

<Fig. 6>

3.4. Contributions of the key RS to EE2 degradation

To qualitatively identify the photogenerated RS and quantitatively assess their contributions to EE2 degradation in the HA contained systems, molecular probes were added into solutions with different experimental conditions to analyze the changes in the photodegradation kinetics of EE2 (Figure S7). HO· and ^{3}HA* were identified as the primary RS dominating EE2 degradation in HA solutions, and the contribution of ^{3}HA* to EE2 degradation in oxygen poor system could be enlarged (Table 3). The photodegradation rate of EE2 in the Milli-Q systems was also inhibited upon addition of IPA, which

could be attributed to the self-sensitized oxidation of EE2 alike the proceedings in the direct photodegradation of fluoroquinolone antibiotics.[17] The phenolic structure was reported as one of the light sensitive groups producing RS,[47] and this mechanism was also involved in the photodegradation of EE2 demonstrated by adding phenol into pure aqueous EE2 as a positive control (Figure S7). Therefore, the self-sensitized oxidation of EE2 was depicted as Eqs. (15) - (19). H_2O_2 scavenging experiments indicated that it was HO· not only produced from the photolysis of H_2O_2 but also from other processes, including hydrogen abstracting from H_2O by the triplet chromophoric dissolved organic matter and quinone-type substances.[26,48,49] The steady-state concentration of HO· and $^1O_2$ in the HA/air system was determined to be 4.83×10^{-15} M and 2.04×10^{-13} M by taking TPA and FFA as selective traps[20,50] (Figure S2 and S3), respectively. The concentration of $^1O_2$ in natural waters and HA contained solutions was typically found to be 2 to 5 orders of magnitude higher than that of HO·.[40,51] The different capacity of HA producing $^1O_2$ and HO· could be explained by its special structure and composition. The contribution of $^1O_2$ to EE2 degradation was always less than 13%, whereas the contribution of ^{3}HA* and HO· was about 22% and 28%, respectively. This result could be attributed to their different reactivity towards EE2 which was measured by a competition kinetics method (Text S3)[30] and shown in Figure S4 and S5. The second-order reaction rate constant between EE2 and HO· was measured to be 1.09×10^{10} M^{-1} s^{-1} and was 3 orders of magnitude higher than that between EE2 and $^1O_2$ (9.71×10^7 M^{-1} s^{-1}). To note that the steady-state concentration of ^{3}HA* was not estimated in this study because the structure of HA used here might be different from that produced by the international humic substance society.[27]

<Table 3>

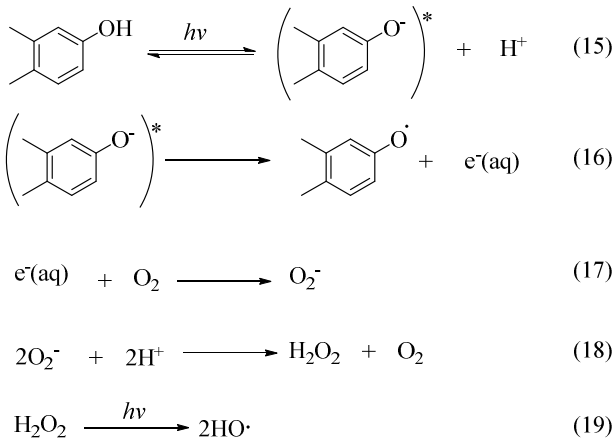

(15)

(16)

$$e^-(aq) + O_2 \longrightarrow O_2^- \quad (17)$$

$$2O_2^- + 2H^+ \longrightarrow H_2O_2 + O_2 \quad (18)$$

$$H_2O_2 \xrightarrow{h\nu} 2HO\cdot \quad (19)$$

3.5. Mechanism for RS formation and EE2 degradation

It was reported that the direct photodegradation of chemicals depends on the light absorption ability of chemicals, intensity of incident light, and quantum yield of excited compounds.[38] Apart from the maximum absorption of EE2 at 292 nm within the emitted light spectrum (pH 8.0), EE2 has an extended light absorption band from 290 to 320 nm shown in Fig.4. The direct photodegradation thus occurred due to the absorption of the photons emitted from this band. High pH value could effectively enhance the light absorption potency and broaden the absorption wavelength range of EE2 (Fig. 4), as a result, more EE2* was formed and degraded.

HO·, ^{3}HA* and $^1O_2$ were identified as the key RS dominating the photodegradation of EE2 in the solutions containing HA (Table 3), and the formation pathways of these RS were depicted as Eqs. (9) - (14). H_2O_2 was determined as one of the main sources of HO· but not the sole. Eq. (12) shows that the formation of H_2O_2 would be increased with pH decreasing if the concentration of superoxide anions remains constant. However, the formation of superoxide anions could be inhibited by the decreased pH value because protonated HA presents lower sensitivity to light.[23] Abundant hydrogen ion at pH 3.0 might contribute to the formation of H_2O_2. Thus, the photodegradation rate of EE2 in the HA containing solutions reached the lowest value at pH 5.0. In oxygen rich systems, the

photodegradation of EE2 could be promoted by DO reacting with excited EE2 and HA. Based on the experimental results, the photodegradation pathways of EE2 and the formation mechanisms of RS in HA solutions regarding the influence of DO and pH were summarized in Fig. 7.

<Fig. 7>

4. Conclusions

EE2 was removed by both direct (< 27%) and indirect photodegradation (> 73%) pathways in HA aqueous solutions. The photodegradation rate of EE2 in Milli-Q water decreased with increased pH in the range of 3.0 ~ 7.0, increased initial concentration of EE2 within 0.8 mg L^{-1} and decreased DO concentration. The deprotonated EE2 could be photodegradated much faster than protonated, and the influence of pH on EE2 photodegradation induced by HA was minor than that on the direct photodegradation of EE2. The direct photodegradtion of EE2 could be enhanced by DO reacting with excited EE2, while the indirect photodegradation of EE2 was promoted by DO reacting with excited HA forming ROS, mainly HO· and $^1O_2$. The concentration of HO· and $^1O_2$ in 5 mg L^{-1} HA solutions was measured to be 4.83×10^{-15} and 2.04×10^{-13} M, and the second-order reaction rate constant of HO· and $^1O_2$ towards EE2 was measured to be 1.09×10^{10} and 9.71×10^7 M^{-1} s^{-1}, respectively. This could perfectly explain $^1O_2$ contributed minor to the photodegradation of EE2 (always < 13%), while HO· and ^{3}HA* were the key contributors. Photogenerated H_2O_2 was identified as one of the sources of HO· but not the unique. Finally, mechanisms responsible for EE2 degradation and RS formation in HA aqueous solutions involving the effect of DO and pH were summarized.

Associated content

Three texts, four tables, and seven figures with further information on materials, experimental

procedures, calculations and additional data were included in the supplementary material.

Acknowledgements

This project was sponsored by the National Natural Science Foundation of China (Grant No. 41401558), Application Fundamental Research Foundation of Yunnan Province, China (Grant No. 2013FA011), Education Department Science Research Foundation of Yunnan Province, China (Grant No. 2014J022), and China Postdoctoral Science Foundation (Grant No. 2014T70887).

References

1 Z. H. Liu, G. N. Lu, H. Yin, Z. Dang and B. Rittmann, *Environ. Sci. Technol.*, 2015, **49**, 5288-5300.

2 B. Huang, B. Wang, D. Ren, W. Jin, J. Liu, J. Peng and X. Pan, *Environ. Int.*, 2013, **59**, 262-273.

3 O. Lee, A. Takesono, M. Tada, C. R. Tyler and T. Kudoh, *Environ. Health Perspect.*, 2012, **120**, 990-996.

4 J. Liu, R. Wang, B. Huang, C. Lin, J. Zhou and X. Pan, *Environ. Pollut.*, 2012, **162**, 325-331.

5 S. Jobling, R. Williams, A. Johnson, A. Taylor, M. Gross-Sorokin, M. Nolan, C. R. Tyler, R. Aerle, E. Santos and G. Brighty, *Environ. Health Perspect.*, 2006, **114**, 32-39.

6 A. Pillon, N. Servant, F. Vignon, P. Balaguer and J.-C. Nicolas, *Anal. Biochem.*, 2005, **340**, 295-302.

7 A. Z. Aris, A. S. Shamsuddin and S. M. Praveena, *Environ. Int.*, 2014, **69**, 104-119.

8 H. Hamid and C. Eskicioglu, *Water Res.*, 2012, **46**, 5813-5833.

9 Y. Zuo, K. Zhang and Y. Deng, *Chemosphere*, 2006, **63**, 1583-1590.

10 Y. Zuo, K. Zhang and S. Zhou, *Environ. Sci.: Processes Impacts*, 2013, **15**, 1529-1535.

11 D. Wang, Y. Li, G. Li, C. Wang, W. Zhang and Q. Wang, *J. Hazard. Mater.*, 2013, **254**, 64-71.

12 M. D. Jürgens, K. I. Holthaus, A. C. Johnson, J. J. Smith, M. Hetheridge and R. J. Williams, *Environ. Toxicol. Chem.*, 2002, **21**, 480-488.

13 A. K. Sarmah, G. L. Northcott and F. F. Scherr, *Environ. Int.*, 2008, **34**, 749-755.

14 G. G. Ying, R. S. Kookana and P. Dillon, *Water Res.*, 2003, **37**, 3785-3791.

15 M. P. Makunina, I. P. Pozdnyakov, Y. Chen, V. P. Grivin, N. M. Bazhin and V. F. Plyusnin, *Chemosphere*, 2015, **119**, 1406-1410.

16 J. Porras, J. J. Fernandez, R. A. Torres-Palma and C. Richard, *Environ. Sci. Technol.*, 2014, **48**, 2218-2225.

17 L. Ge, J. Chen, X. Wei, S. Zhang, X. Qiao, X. Cai and Q. Xie, *Environ. Sci. Technol.*, 2010, **44**, 2400-2405.

18 E. De Laurentiis, S. Buoso, V. Maurino, C. Minero and D. Vione, *Environ. Sci. Technol.*, 2013, **47**, 14089-14098.

19 N. J. Turro, V. Ramamurthy and J. C. Scaiano, Wiley Online Library, 2012.

20 W. Song, S. Yan, W. J. Cooper, D. D. Dionysiou and K. E. O'Shea, *Environ. Sci. Technol.*, 2012, **46**, 12608-12615.

21 E. Caupos, P. Mazellier and J. P. Croue, *Water Res.*, 2011, **45**, 3341-3350.

22 W. Grzybowski and J. Szydłowski, *Chemosphere*, 2014, **111**, 13-17.

23 L. A. Molot, J. J. Hudson, P. J. Dillon and S. A. Miller, *Aquat. Sci.*, 2005, **67**, 189-195.

24 P. Westerhoff, Y. Yoon, S. Snyder and E. Wert, *Environ. Sci. Technol.*, 2005, **39**, 6649-6663.

25 L. S. Lee, T. J. Strock, A. K. Sarmah and P. S. C. Rao, *Environ. Sci. Technol.*, 2003, **37**, 4098-4105.

26 S. E. Page, W. A. Arnold and K. McNeill, *Environ. Sci. Technol.*, 2011, **45**, 2818-2825.

27 J. E. Grebel, J. J. Pignatello and W. A. Mitch, *Water Res.*, 2011, **45**, 6535-6544.

28 G. V. Buxton, C. L. Greenstock, W. P. Helman and A. B. Ross, *J. Phys. Chem. Ref. Data*, 1988, **17**, 513-886.

29 W. R. Haag, E. Gassman and A. Braun, *Chemosphere*, 1984, **13**, 631-640.

30 J. Wenk, U. von Gunten and S. Canonica, *Environ. Sci. Technol.*, 2011, **45**, 1334-1340.

31 A. Leifer, American Chemical Society, 1988.

32 P. Mazellier, L. Méité, J.D. Laat, *Chemosphere*, 2008, **73,** 1216-1223.

33 G. Grabner, G. Köhler, J. Zechner and N. Getoff, *Photochem. Photobiol.*, 1977, **26**, 449-458.

34 R. R. Chowdhury, P. Charpentier and M. B. Ray, *Ind. Eng. Chem. Res.*, 2010, **49**, 6923-6930.

35 Y. Chen, K. Zhang and Y. Zuo, *Sci. Total Environ.*, 2013, **463**, 802-809.

36 M. Barakat, H. Schaeffer, G. Hayes and S. Ismat-Shah, *Appl. Catal., B*, 2005, **57**, 23-30.

37 K. Aguilar, A. Garvin, E. Azuara and A. Ibarz, *Food Res. Int.*, 2015, **71**, 165-173.

38 M. Czaplicka, *J. Hazard. Mater.*, 2006, **134**, 45-59.

39 B. Liu and X. Liu, *Sci. Total Environ.*, 2004, **320**, 269-274.

40 D. Zhang, S. Yan and W. Song, *Environ. Sci. Technol.*, 2014, **48**, 12645-12653.

41 R. B. Young, D. E. Latch, D. B. Mawhinney, T.-H. Nguyen, J. C. Davis and T. Borch, *Environ. Sci. Technol.*, 2013, **47**, 8416-8424.

42 E. M. L. Janssen, P. R. Erickson and K. McNeill, *Environ. Sci. Technol.*, 2014, **48**, 4916-4924.

43 D. M. Leech, M. T. Snyder and R. G. Wetzel, *Sci. Total Environ.*, 2009, **407**, 2087-2092.

44 J. A. Marinsky and J. Ephraim, *Environ. Sci. Technol.*, 1986, **20**, 349-354.

45 A. Rubio-Clemente, R. A. Torres-Palma and G. A. Peñuela, *Sci. Total Environ.*, 2014, **478**, 201-225.

46 L. Chen, C. Shen, M. Zhou, X. Tang and Y. Chen, *Environ. Sci. Pollut. Res.*, 2013, **20**, 1842-1848.

47 S. P. Wu, J. Schwab, B. Y. Yang and C. S. Yuan, *J. Photochem. Photobiol., A*, 2015, **309**, 55-64.

48 M. M. Dong and F. L. Rosario-Ortiz, *Environ. Sci. Technol.*, 2012, **46**, 3788-3794.

49 A. Pochon, P. P. Vaughan, D. Gan, P. Vath, N. V. Blough and D. E. Falvey, *J. Phys. Chem. A*, 2002, **106**, 2889-2894.

50 S. E. Page, W. A. Arnold and K. McNeill, *J. Environ. Monit.*, 2010, **12**, 1658-1665.

51 F. al Housari, D. Vione, S. Chiron and S. Barbati, *Photochem. Photobiol. Sci.*, 2010, **9**, 78-86.

Table 1. Selected physiochemical properties of 17α-Ethynylestradiol

Estrogen	Molecular weight ($g\ mol^{-1}$)	Water solubility[14] (20 °C, $mg\ L^{-1}$)	lgK_{ow}[24]	lgK_{oc}[25]	pK_a[25]
EE2 ($C_{20}H_{24}O_2$)	296.40	4.80	3.67	2.99	10.5

Table 2 Observed and corrected degradation rate constants and half-lives of EE2 at different concentration of HA

HA concentration ($mg\ L^{-1}$)	k_{obs} (h^{-1})	k_{cor} (h^{-1})	Contribution of HA (%)	$t_{1/2}$ (h)
0	0.0193 ± 0.0003	-	-	35.9
2	0.0547 ± 0.0006	0.0191	65	12.7
5	0.0739 ± 0.0004	0.0183	75	9.4
10	0.0731 ± 0.0003	0.0179	76	9.5
15	0.0674 ± 0.0005	0.0172	74	10.3
20	0.0665 ± 0.0002	0.0164	75	10.4

Table 3. Degradation rate of EE2 in different irradiated solutions

	Milli-Q in air		HA in air		Milli-Q pH 8.0		HA pH 8.0	
	pH 8.0	pH 11.0	pH 8.0	pH 11.0	N_2	O_2	N_2	O_2
No-SCA	0.0193 (± 0.0005)	0.4250 (± 0.0005)	0.0739 (± 0.0006)	0.5174 (± 0.0055)	0.0178 (± 0.0006)	0.0351 (± 0.0007)	0.0539 (± 0.0018)	0.1674 (± 0.0012)
IPA	0.0175 (± 0.0007)	0.3316 (± 0.0052)	0.0533 (± 0.0006)	0.3543 (± 0.0032)	0.0177 (± 0.0004)	0.0316 (± 0.0028)	0.0461 (± 0.0011)	0.1125 (± 0.0008)
FFA	0.0201 (± 0.0005)	0.4311 (± 0.0021)	0.0649 (± 0.0004)	0.5032 (± 0.0075)	0.0182 (± 0.0015)	0.0345 (± 0.0006)	0.0494 (± 0.0009)	0.1564 (± 0.0013)
SA	0.0168 (± 0.0008)	0.3435 (± 0.0032)	0.0577 (± 0.0005)	0.4568 (± 0.0086)	0.0164 (± 0.0009)	0.0337 (± 0.0005)	0.0398 (± 0.0008)	0.1538 (± 0.0016)
CAT	0.0210 (± 0.0004)	0.4568 (± 0.0009)	0.0647 (± 0.0011)	0.4946 (± 0.0061)	0.0187 (± 0.0007)	0.0359 (± 0.0008)	0.0526 (± 0.0012)	0.1584 (± 0.0007)

* ± error represents at the 0.95 confidence level

Fig. 1 Stability of EE2 in dark and under the irradiation of the simulated sunlight

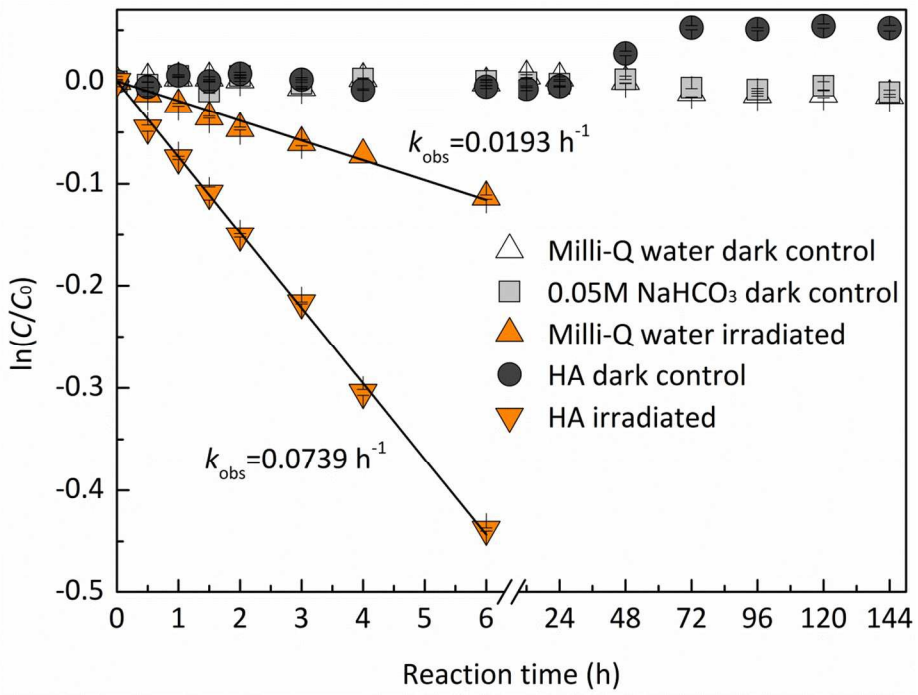

Fig. 2 Dependence of the direct photodegradation of EE2 on the initial concentration

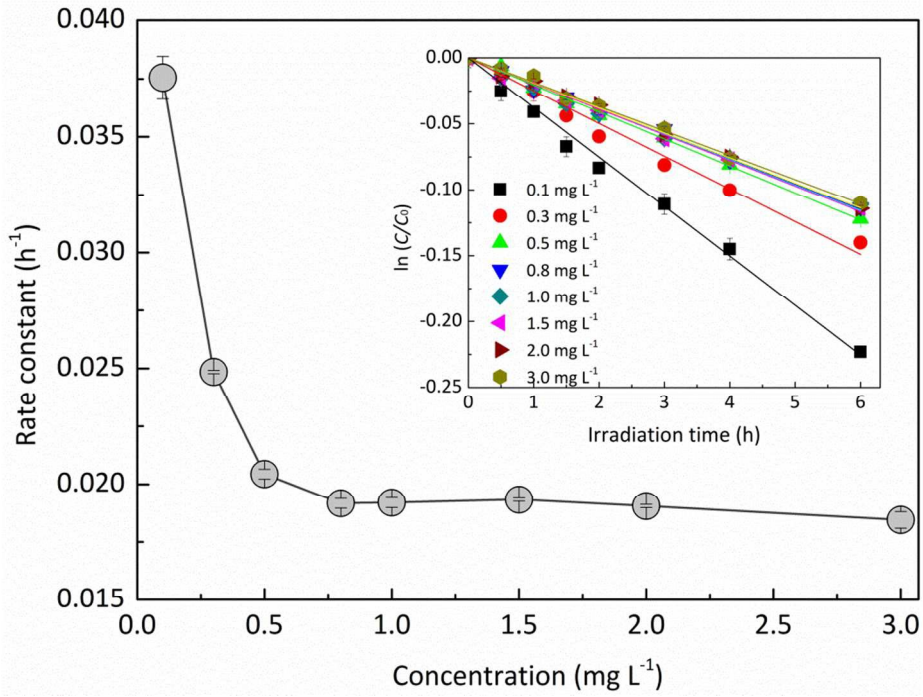

Fig. 3 Influence of pH on the speciation and the direct photodegradation of EE2

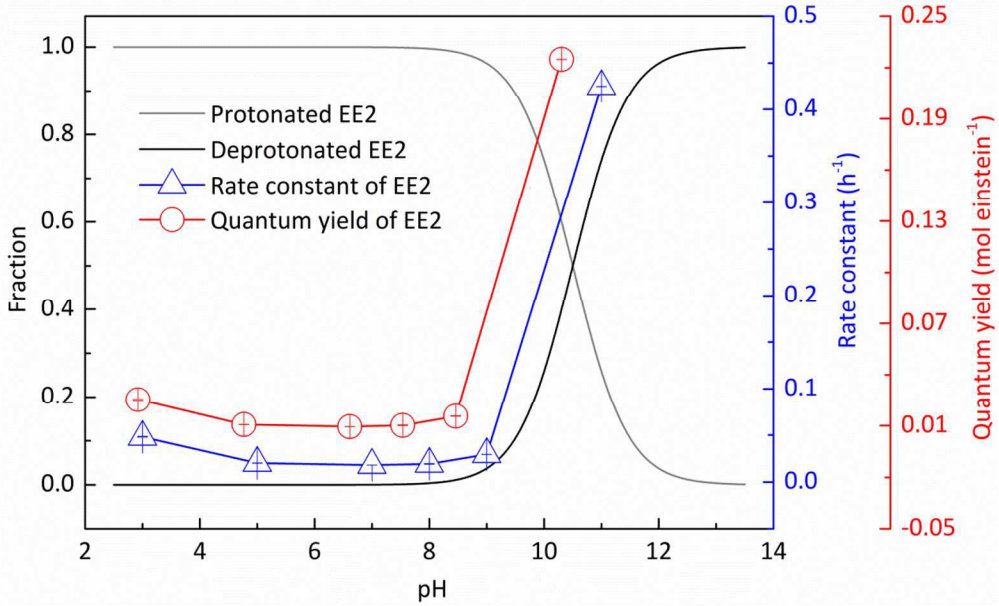

Fig. 4 Absorption characteristics of EE2 aqueous solution (3.0 mg L^{-1}) under different pH conditions

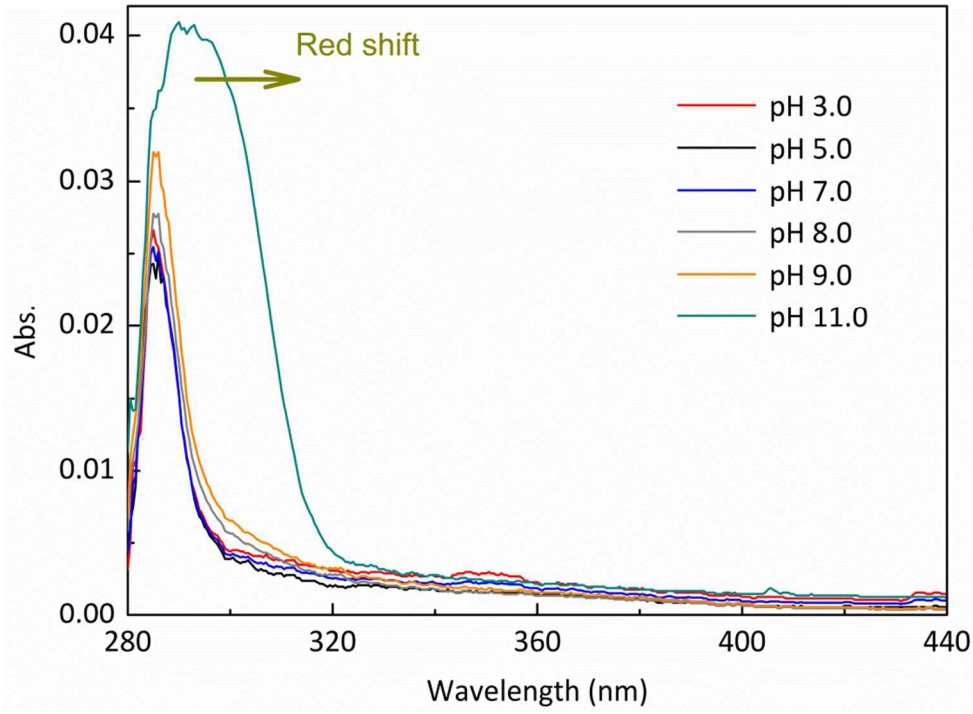

Fig. 5 Photodegradation of EE2 in 5.0 mg L^{-1} HA solutions at different pH values

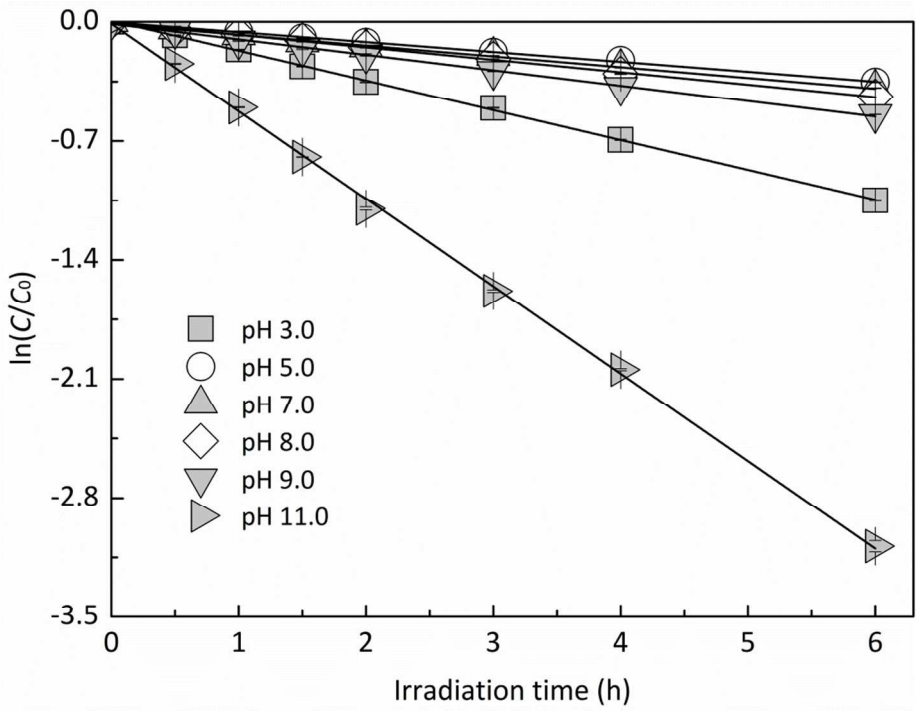

Fig. 6 Effects of DO on the photodegradation of EE2 (a) in Milli-Q water (b) in HA aqueous solution

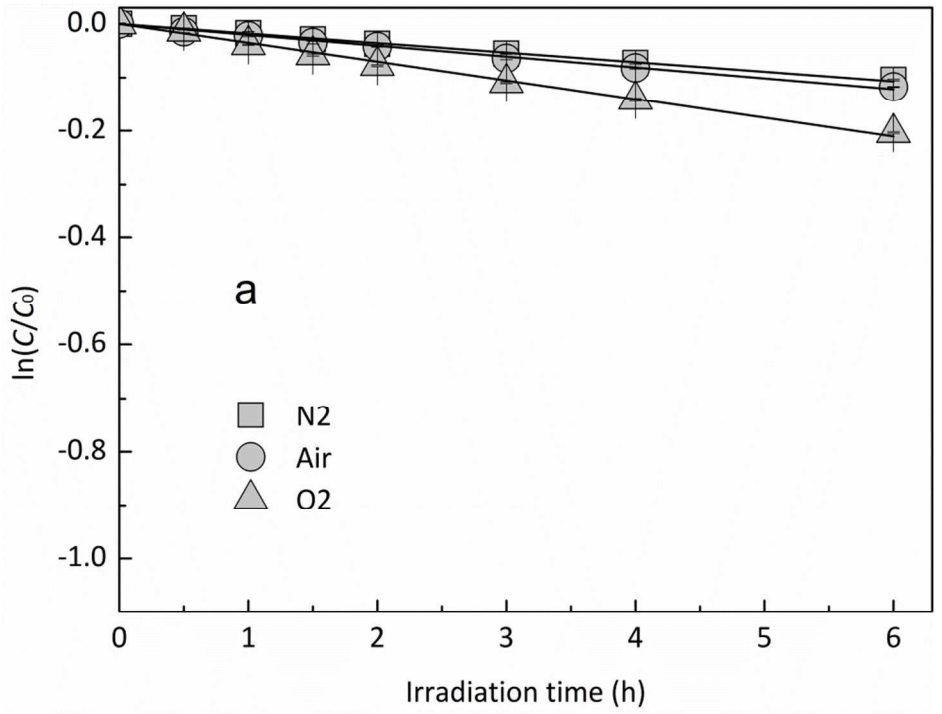

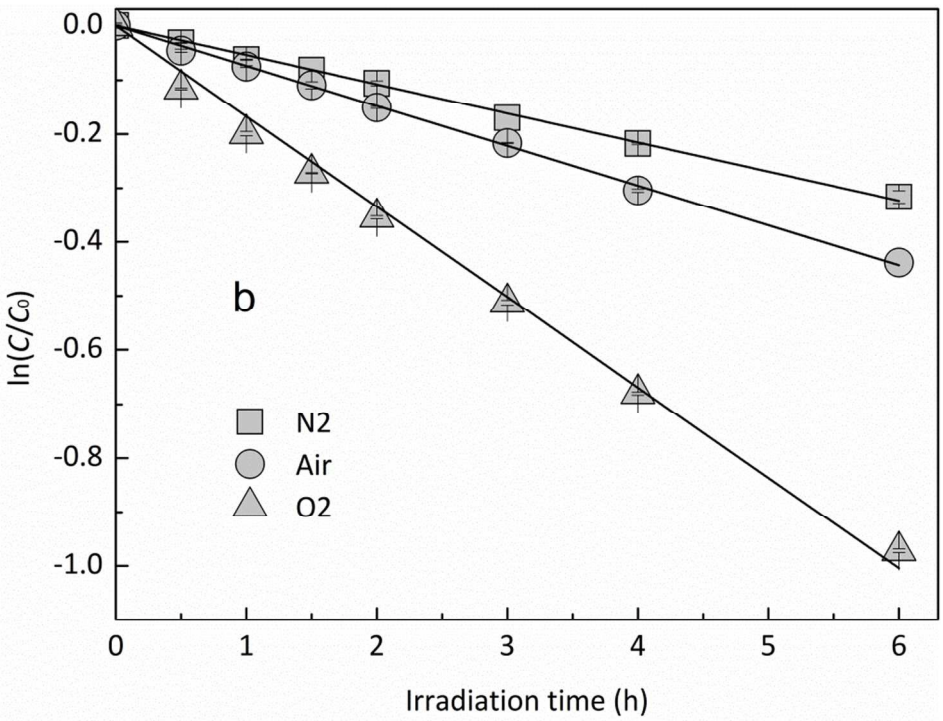

Fig. 7 Mechanism for EE2 photodegradation and RS formation in HA aqueous solution